ACS APPLIED MATERIALS & INTERFACES

Research Article

Cite This: ACS Appl. Mater. Interfaces 2019, 11, 38084−38091

www.acsami.org

Versatile Electronic Skins with Biomimetic Micronanostructures Fabricated Using Natural Reed Leaves as Templates

Yu-Qing Liu,[†] Jia-Rui Zhang,[†] Dong-Dong Han,[†] Yong-Lai Zhang,[*,†] and Hong-Bo Sun[‡]

[†]State Key Laboratory of Integrated Optoelectronics, College of Electronic Science and Engineering, Jilin University, 2699 Qianjin Street, Changchun 130012, China

[‡]State Key Laboratory of Precision Measurement Technology & Instruments, Department of Precision Instrument, Tsinghua University, Haidian District, Beijing 100084, China

Supporting Information

ABSTRACT: Versatile electronic skin devices that enable detection of multimodal signals have revealed great potential for human health monitoring. To make a versatile electronic skin, hierarchical micronanostructures are essential to obtain improved sensing performance and multisignal detection capability. However, current strategies for developing a nanostructured electronic skin usually involve complex procedures, harsh experimental conditions, and the use of expensive equipment, which limit its practical applications. In this paper, we reported the fabrication of a multifunctional wearable electronic skin with hierarchical micronanostructures by using natural reed leaves as templates. The capacitive-type electronic skin is fabricated by double-sided coating of Au electrodes on an artificial polydimethylsiloxane reed leaf that is duplicated from natural reed leaves via soft lithography. The electronic skin features a very simple device structure yet high sensing performance. It permits multimodal signal detection, including that of pressure, deformation, and proximity, and can serve as surface-enhanced Raman scattering substrates for the detection of metabolites in sweat because of the formation of plasmonic structures. The versatile electronic skin can be attached to the human skin, and it enables effective monitoring of multiphysiological signals, revealing great potential for cutting-edge applications, such as human health monitoring.

KEYWORDS: *versatile sensor, electronic skin, reed leaf, biomimetic structure, soft lithography*

INTRODUCTION

Electronic skins[1−3] are promising soft electronics that hold great potential for cutting-edge applications in human health monitoring,[4−8] medical treatments,[9−11] medical implants,[12,13] human−machine interfaces,[14−16] and robotic tactility.[17−19] Electronic skins generally consist of input/output devices for human interaction and coupled circuits for information processing, in which the sensor elements play a critical role in their performance. At present, flexible sensors that can detect multiforms of physical, chemical, and physiological signals have been successfully developed based on different sensing mechanisms. For instance, resistive-type pressure sensors that feature softness, flexibility, and stretchability have been fabricated as electronic skins for detecting tiny forces such as wrist pulses and acoustic vibrations at throat.[20−24] Capacitive-type sensors that consist of a pair of electrodes and a dielectric layer enable sensitive detection of pressure, strain, and proximity.[25−27] Thermal-sensitive fluid-embedded flexible elastomers have been prepared as soft, reconfigurable, and repairable electronics for monitoring temperature and body motion.[28−30] The recent success of flexible sensors has resulted in the rapid progress of wearable electronic skins.

To make a versatile and high-performance electronic skin, hierarchical micronanostructures are essential to obtain improved sensing properties and multisignal detection capability. Especially, with the rapid advances of micro-nanofabrication technologies in the recent years, sensors that feature hierarchical micronanostructures have been successfully fabricated through various "top-down" and "bottom-up" approaches.[31−39] For instance, nanostructured pressure sensors with high sensitivity and low detection limit have been successfully developed based on pyramid/microdome arrays,[35,37] gratings,[33] and interlocking microstructures.[32] Notably, these structured pressure sensors have demonstrated much higher sensing performance as compared with those fabricated based on planar substrates. However, current strategies for developing nanostructured electronic skins usually involve complex procedures, harsh experimental conditions, and the use of expensive equipment, which limit their practical applications. Actually, after ultralong time evolution, natural materials have already possessed sophisticated structures that impart superwettability, structural colors, mechanical strength, and various survival skills.[40,41] Using natural materials as templates, biomimetic surfaces with micronanostructures comparable to their natural models can be readily prepared

Received: August 8, 2019
Accepted: September 24, 2019
Published: September 24, 2019

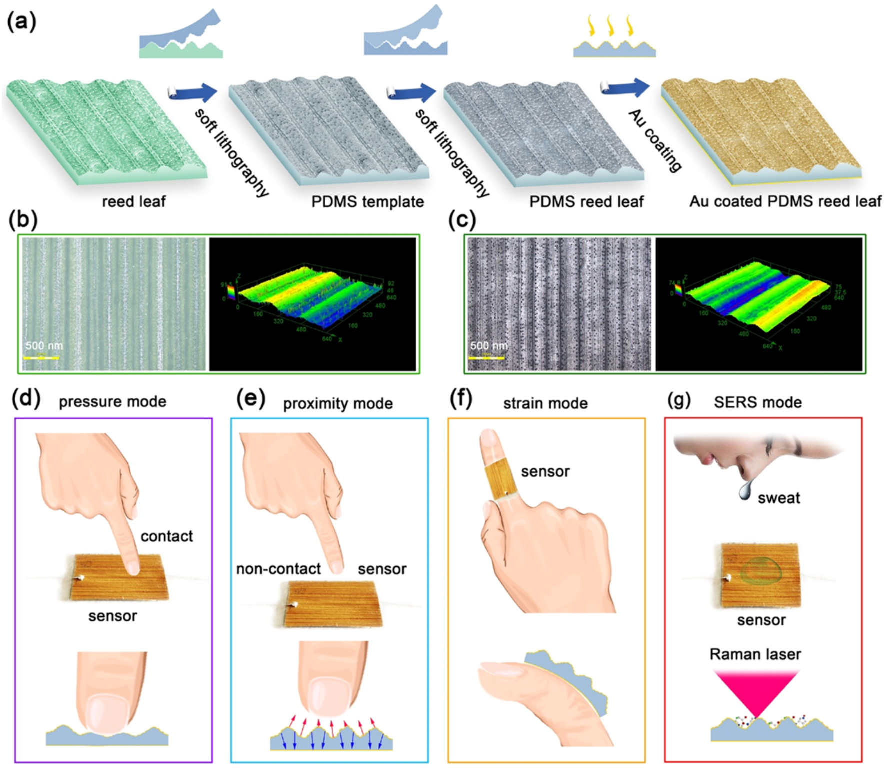

Figure 1. (a) Schematic illustration for the fabrication of the micronanostructured capacitive sensor using a natural reed leaf as the template. (b) Laser scanning confocal microscopy (LSCM) images and the 3D version of the natural reed leaf. (c) LSCM images and the 3D version of the PDMS reed leaf prepared via twice duplication. (d−g) Schematic illustration of different sensing modes, (d) pressure mode, (e) proximity mode, (f) strain mode, and (g) SERS mode.

based on artificial materials through a simple soft lithography process.[42−49] Some pioneer works have proven the feasibility of producing bionic pressure sensors by duplicating natural templates such as lotus,[44] mimosa,[46] and *E. aureum* leaves.[49] Nevertheless, the reported works are limited to resistive-type pressure sensors. Currently, considering the diversity of micronanostuctures that exist in natural materials, the bionic templating strategy has not revealed its full potential for fabricating nanostructured pressure sensors, especially, for developing versatile electronic skins.

In this paper, we reported a capacitive-type versatile electronic skin with biomimetic micronanostructures using natural reed leaves as templates. Instead of using a sandwiched device structure, we fabricated the capacitive-type sensor by coating Au electrodes on both the front side and the back side of an artificial polydimethylsiloxane (PDMS) reed leaf that is duplicated from natural reed leaves via twice soft lithography. The resultant electronic skin permits multimodal signal detection, including that of pressure, bending, and proximity, and can serve as surface-enhanced Raman scattering (SERS) substrates for the detection of the metabolites in sweat, revealing great potential for human health monitoring.

■ EXPERIMENTAL METHODS

Fabrication of PDMS Artificial Reed Leaves. Fresh reed leaves were obtained from a lakeside in the campus of Jilin University. The duplication of reed leaves was performed by twice soft lithography. In the first duplication process, a mixture of the PDMS base and a curing agent (Sylgard 184 silicone elastomer kit, Dow Corning Corporation, Auburn, MI, USA) with a mass ratio of 10:1 was poured into the reed leaf mold and cured at 85 °C for 2 h. The peeled-off PDMS replica with a reverse reed leaf structure was used as the template for the second duplication process. To facilitate the demolding process, we modified this PDMS template with fluoroalkylsilane. Artificial PDMS reef leaves can be fabricated after the second duplication process.

Fabrication of the Capacitive Sensor. The front and back sides of PDMS reed leaves were treated with O_2 plasma for 5 min to generate more hydroxyl groups. After that, it was modified with mercaptopropyltrimethoxysilane (MPTS) to graft sulfydryl groups on the surface. The capacitive sensors were fabricated by physical vapor deposition (PVD) coating of a gold layer on both the front and back sides of the PDMS reed leaf. Deposition rate of gold was about 0.15 nm/s, and the thickness of the Au layer is 20 nm.

Characterization. The capacitance was recorded by using a GW INSTEK LCR-6200 meter. Scanning electron microscopy (SEM) images were obtained using a JEOL JSM-7500 field-emission scanning electron microscope. Raman spectroscopy was performed by using the HOARIBA, LabRAM HR Evolution instrument. The three-dimensional (3D) surface profiles were measured using a laser scanning confocal microscope (LSCM, OLS4100, Japan).

■ RESULTS AND DISCUSSION

Fabrication of the Capacitive Sensor. Reed is a kind of a very common plant that grows near wetlands. To maintain a wet environment to survive, its leaves show anisotropic and hierarchical micronanostructures. In this way, water droplets can easily roll along its leaf vein to its root. The reed leaf is a typical model for preparing artificial superhydrophobic surfaces that feature anisotropic wettability. We prepared the micronanostructured capacitive sensor using a natural reef leaf as the template. Figure 1a shows the schematic illustration of the fabrication procedure. First, a fresh reed leaf was attached to a flat glass substrate. Soft lithography processing was performed to duplicate a PDMS template with the reverse structure of the reed leaf. Then, to facilitate the demolding in the subsequent

DOI: 10.1021/acsami.9b14135
ACS Appl. Mater. Interfaces 2019, 11, 38084−38091

duplication, the PDMS template was modified with fluoroalkylsilane. We performed the second soft lithography and peeled off the PDMS reed leaf from the PDMS template for device fabrication. To form a capacitive device structure, we coated a thin layer of Au on both the front side (with reed leaf structure) and the back side (planar structure) through a PVD method. To improve the interface adhesion between PDMS and the Au layer, the PDMS reed leaf was treated with O_2 plasma and modified with MPTS. The device features a very simple sandwich structure, in which the two Au layers functionalized as electrodes and the interlayer PDMS served as a dielectric layer. We further characterized the natural reed leaf and the PDMS reed leaf with a laser scanning confocal microscope (Figure 1b−e). The natural reed leaf shows a hierarchical and anisotropic micronanostructure. Periodically distributed microgrooves with an average period of 150 μm can be clearly identified. Besides, randomly distributed micropapillae can be observed along the grooves. The 3D version shows the nonplanar structure of the reed leaf. Interestingly, after twice soft lithography, the reed leaf structure can be well inherited by the PDMS replica. As shown in Figure 1c,e, similar structures including the microgrooves and randomly distributed micropapillae can be observed on the PDMS surface. The presence of such microstructures is quite helpful for promoting the sensing performance and the formation of plasmonic structures after Au coating. Featuring a unilateral microstructure, the Au-coated PDMS reed leaf can functionalized as a versatile sensor for detecting multiforms of signals. Figure 1d−g shows different sensing models. As a capacitive pressure sensor, it can detect various pressures because of the capacitance changes under pressing (Figure 1d). The mutual capacitance change is very sensitive to the location of the finger; thus, the sensor can detect finger proximity through a noncontact model (Figure 1e). Besides, it enables monitoring body motions, for instance, the bending of a finger because the strain can also alter its capacitance (Figure 1f). Interestingly, our Au-coated PDMS reed leaf can serve as a highly efficient SERS substrate for detecting the metabolites in sweat because of the formation of plasmonic structures (Figure 1g). Because different sensing modes work through different mechanisms, different signals can be distinguished. The multisignal sensing capability makes the Au-coated PDMS reed leaf an ideal sensor for human health monitoring.

Characterization of the Capacitive Sensor. To obtain deep insight into the hierarchical micronanostructures of both natural reed leaves and their PDMS replicas, we characterized these samples by SEM. Figure 2 shows the SEM images of a natural reed leaf, the PDMS read leaf, and the Au-coated PDMS reed leaf. The SEM image of a natural reed leaf clearly shows the microgrooves and the micropapillae, similar to that observed from the LSCM images. The magnified SEM image shows that the surface of the reed leaf is quite rough. In addition to the micropapillae with a size of 10−20 μm, there are plenty of coiled nanofibers (Figure 2b). After twice soft lithography, the PDMS replica shows a similar structure (Figure 2c). Both the microgrooves and the micropapillae were inherited from the natural template. Nevertheless, the coiled nanofibers are absent on the surface of the PDMS replica (Figure 2d). This phenomenon is quite easy to understand. For nanoscale coiled fibers, it is quite difficult to demold. We have performed twice soft lithography, and during twice demolding processes, all the coiled nanofibers are lost. It is

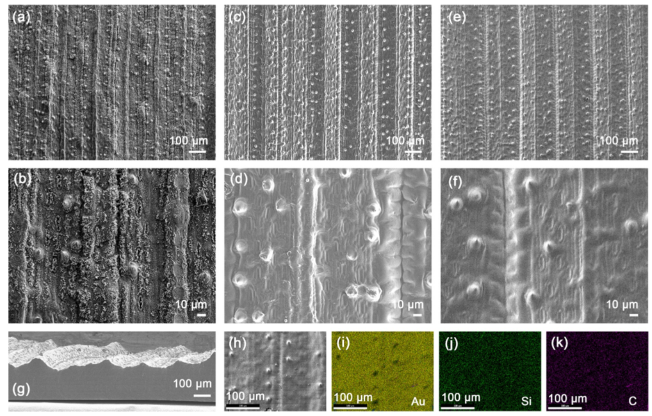

Figure 2. (a) SEM image of the natural reed leaf. (b) Magnified SEM image of the natural reed leaf. (c) SEM image of the PDMS reed leaf. (d) Magnified SEM image of the PDMS reed leaf. (e) SEM image of the Au-coated PDMS reed leaf. (f) Magnified SEM image of the Au-coated PDMS reed leaf. (g) Sectional view of the Au-coated PDMS reed leaf. (h−k) Elemental maps of Au, Si, and C.

worth pointing out that for a resistive-type pressure sensor, the nanostructure may be quite important to acquire high sensitivity, especially at low-pressure regions. While for a capacitive sensor, the presence of coiled nanofibers is meaningless because the deformation of coiled nanofibers may induce an unobvious capacitance change but increase the risk of detachment of these fragile nanofibers during frequent pressing. After coating a thin layer of Au, the surface morphology almost remains unchanged. Figure 2e,f shows the SEM images of the Au-coated PDMS reed leaf; it is very similar to the one without Au coating. The sectional-view SEM image shows that the PDMS reed leaf is about 200 μm in thickness. The depth of the microgrooves is about 80 μm (Figure 2g). Considering the softness, elastic resistance, and the robustness for demolding, the PDMS thickness is an optimized parameter. To confirm the presence of the Au layer, Au, Si, and C element maps of the Au-coated PDMS were collected. As shown in Figure 2h−k, the distribution of Au, Si, and C coating is quite uniform, indicating the presence of a continuous Au layer on the PDMS substrate. The thickness of the Au layer is ∼20 nm. The thickness of the Au layer may influence the sensor performance. If the Au layer is too thin, the gold electrodes may be discontinuous, whereas a much thicker Au layer may lower the sensitivity of the sensor because it may cover some of the nanostructures.

Sensing Performance. The capacitive sensing performances of our sensor was quantitatively investigated. The sensitivity (S) of our capacitive sensor is calculated by the following equation

$$S = d(\Delta C/C_0)/dP$$

where ΔC is the capacitance change under a certain pressure, C_0 is the pristine capacitance of the sensor, and P is the applied pressure. Theoretically, the sensor performance does not depend on the size of the sensor. To choose a suitable sensor size for practical detection, we used sensors of ∼0.8 × 1 cm for all the subsequent tests. Figure 3a shows the sensitivity curve of the Au-coated PDMS reed leaf. In the low-pressure range, from 0 to 1 kPa, the capacitive sensor shows a quasilinear dependence sensitivity on the pressure. The sensitivity is calculated to be ∼0.6 kPa^{-1}. The high sensitivity in the low-

DOI: 10.1021/acsami.9b14135
ACS Appl. Mater. Interfaces 2019, 11, 38084−38091

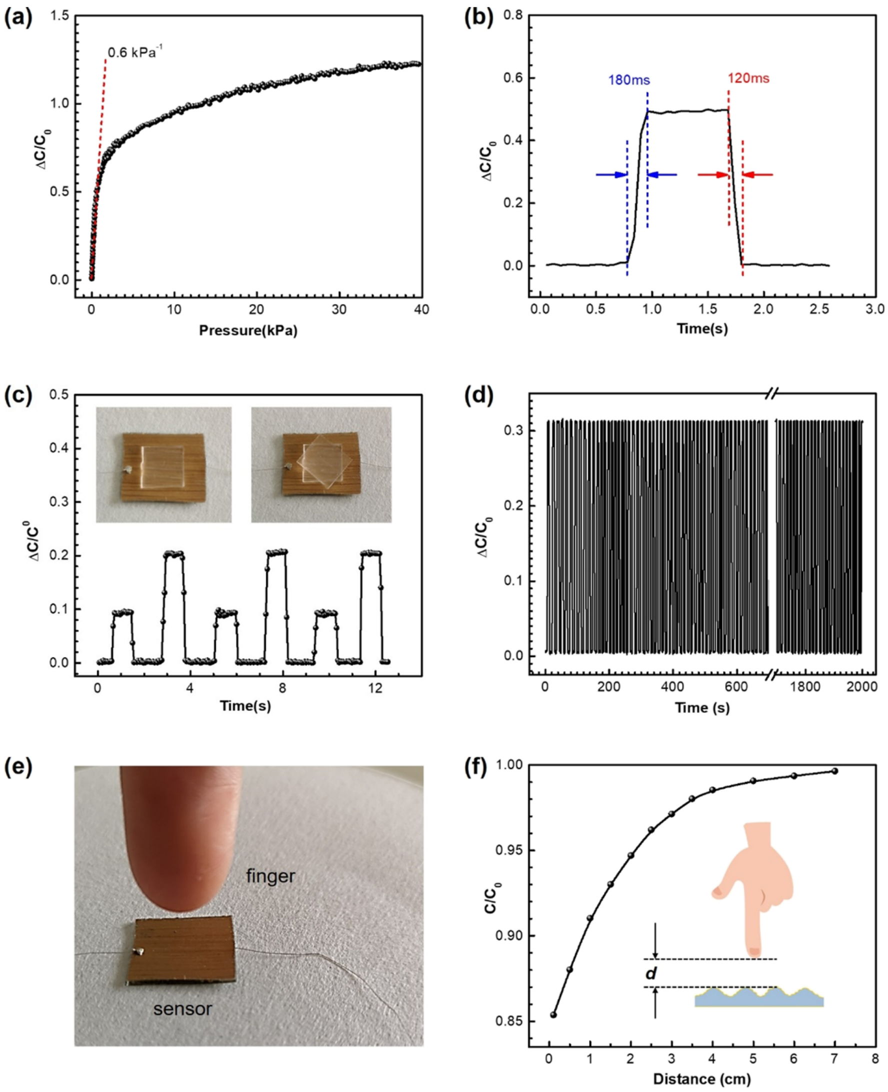

Figure 3. (a) Sensitivity of the capacitive sensor. (b) Response and recovery time of the capacitive sensor. (c) Relative capacitance variations of the capacitive sensor under subtle pressures of one and two PDMS slices. (d) Long-term stability of the sensing paper during repeated pressure loading–unloading cycles. (e) Photograph of the proximity sensing measurement. (f) Capacitive changes vs the distance between the sensor and the finger.

pressure region can be attributed to the presence of microgrooves and the micropapillae. Such microstructures can deform easily under tiny pressure and alter the capacitance of the device. When larger pressure is applied, the sensitivity decreased accordingly. This can be ascribed to the resistance of the PDMS slice. Figure 3b shows response and recovery properties of the capacitive sensor. Within a single pressure loading and unloading cycle, the response time and recovery time are measured to be 180 and 120 ms, respectively. Taking advantage of the high sensitivity in the low-pressure range, the sensing paper can detect subtle pressures, such as a PDMS slice (~50 Pa, Figure 3c). The relative capacitance variations corresponding to one and two PDMS slices also indicate the linear behavior of the sensitivity in the low-pressure range. The detection limit in the mode of pressure sensing is measured to be ~4.5 Pa (Figure S1). The capacitive sensor is reliable and repeatable for detecting different pressures. Moreover, during repeated pressure loading–unloading cycles, our capacitive sensor demonstrates good stability and durability (Figure 3d). The capacitance change is repeatable and stable without performance degradation, indicating the robustness of our sensor for long-term usage.

In addition to the contact-mode pressure detection, the capacitive sensor also enables proximity sensing (Figure 3e). Figure S2a shows the schematic illustration of the detection mechanism. The sensor is like a parallel plate capacitor, where two types of capacitance, self-capacitance (C_s) and mutual capacitance (C_m) coexist in the device. The C_s is the capacitance of the Au electrode with respect to ground, which can be ignored. C_m is the capacitance between the two Au electrodes, which is measured in our experiments. When external grounded conductors, for instance, a finger or a metal rod, gradually approach the sensor, there will be generated a parasitic capacitance (C_p) between the finger (metal rod) and the electrode, which is related to the distance between them. With the approaching of the finger, the electric field between the two electrodes will be disturbed and partially shunted by the finger, thus reducing the C_m. As the distance decreases, the C_p increases, and the C_m further decreases accordingly. To quantitatively investigate the proximity detection capability, we

DOI: 10.1021/acsami.9b14135
ACS Appl. Mater. Interfaces 2019, 11, 38084−38091

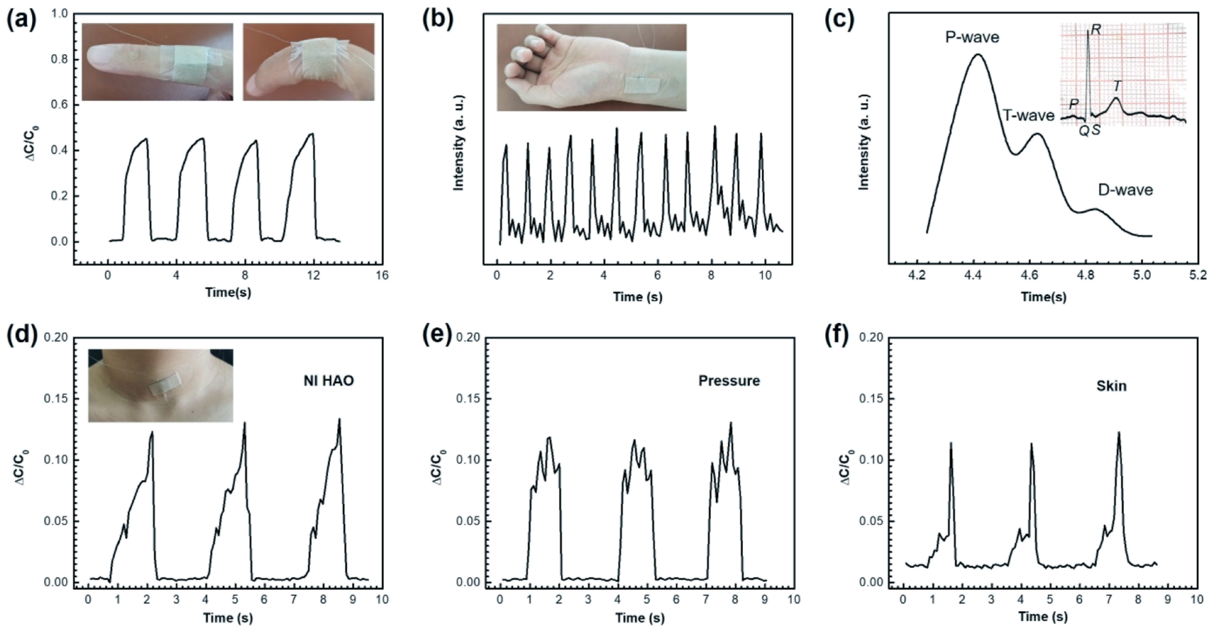

Figure 4. (a) Capacitive response of the sensor during the bending and unbending of a finger for four cycles. The inset shows photographs of a finger wearing the pressure sensor at the knuckle. (b) real-time recording of wrist pulses based on the capacitive pressure sensors. The inset shows photograph of a wrist wearing the pressure sensor. (c) Magnified view of a single pulse. The inset is the commercial electrocardiogram result. (d−f) Capacitance changes to the acoustic vibrations of different words, (d) Chinese word "NI HAO". The inset is the photograph of the sensor attached to the throat, (e) "pressure", and (f) "skin".

changed the distance between a hovering finger and the sensor and recorded the capacitance changes. Figure 3f shows the dependence of capacitance changes on the distance. When the finger approaches the sensor, a part of the fringing electric field can be absorbed, leading to the negative change in capacitance. The detectable distance is measured to be ∼7 cm. With the decrease of the distance, the capacitance of the sensor decreased obviously. For instance, when the distance is 6 cm, 4% capacitance decrease can be detected. When the distance decreased to ∼1 mm, the capacitance decreased to 85%. Using a grounded metal rod as an alternative, the sensor shows a similar proximity sensing property (Figure S2b). Nevertheless, in the case of a statically neutralized metal rod, it shows a much smaller capacitance change (Figure S2c). The proximity sensing capability makes the capacitive sensor smarter than those resistive-type ones, especially for applications in robotic tactility. Besides, the sensor also enables detection of bending deformation through a strain-sensing mode. Nevertheless, because the Au electrode is not stretchable, the sensor is only workable within a small bending angle. Figure S3 shows the schematic illustration and sensitivity in the strain mode. In a small bending curvature range (e.g., from 0 to 0.5 cm^{-1}), the sensitivity is calculated to be 0.7 cm. The detection limit in the mode of strain sensing is measured to be ∼0.2 cm^{-1} (Figure S4). To make a comprehensive comparison with other similar sensors reported elsewhere, we summarized the sensing performance of some typical capacitive sensors in Table S1, in which our sensor shows multimode detection capability and reasonable performance.

Human Health Monitoring Using the Capacitive Sensor as the Electronic Skin. The Au-coated PDMS reed leaf is thin, flexible, and soft, and thus, it can be employed as a versatile electronic skin for human health monitoring. We wear the capacitive sensor over the knuckle of a finger with the help of a band-aid. The sensor enables sensitive detection of finger motions such as bending and unbending motions (Figure 4a). Besides, we also attached the capacitive sensor onto the radial artery of a human wrist for real-time detection of wrist pulses. Figure 4b shows the periodic capacitance change under the pressure of pulses, indicating the reproducible waveforms of wrist pulses. The pulse rates were measured to be ∼70 beats min^{-1}. The enlarged wrist pulse waveform is shown in Figure 4c; three typical peaks, including the percussion wave (P-wave), tidal wave (T-wave), and diastolic wave (D-wave), can be well distinguished. We further compared the pulse waveform with a commercial electrocardiogram sensor (inset of Figure 4c). These results are in good agreement with each other, indicating that our pressure sensor is effective.

In addition to motion and pulse detection, the capacitive sensor is also capable of recognizing human voice by detecting the acoustic vibrations at the throat. In our experiment, a capacitive sensor was attached to the throat position (inset of Figure 4d). We measured the capacitance change when pronouncing the words "NI HAO" (a Chinese word), "Pressure", and "Skin" three times (Figure 4d−f). The capacitive sensor can discriminate the vibration patterns when different words are pronounced. Moreover, the signals of these vibration patterns are reliable when these words were repeated three times.

Unlike those pressure sensors that can detect only physical signals, our sensor can also functionalize as SERS-active substrates for detecting chemical/and biological signals from the metabolites. It is well-known that the dominant enhancement mechanism of SERS can be ascribed to the highly enhanced electric field, also called "hot spot", at the surface of metal nanostructures because of the excitation of localized surface plasmon resonance. According to this design principle, various metallic micronanostructures have been readily fabricated and employed as SERS substrates for highly

DOI: 10.1021/acsami.9b14135
ACS Appl. Mater. Interfaces 2019, 11, 38084−38091

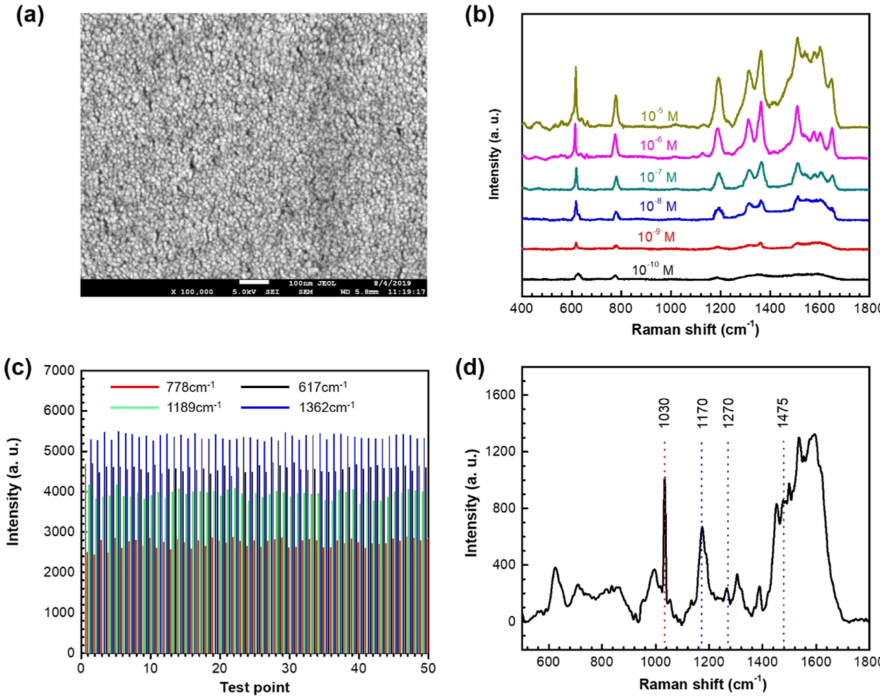

Figure 5. (a) SEM image of the surface of Au-coated PDMS reed leaf. (b) SERS spectra of R6G with different concentrations. (c) Reproducibility of the SERS signals tested over 50 points. (d) SERS spectrum of human sweat after exercise.

sensitive label-free detection of analytes at a very low concentration. Natural materials have already demonstrated various micronanostructures. After silver or gold coating, plasmonic structures would form, which can serve as SERS substrates. In our previous works, we have confirmed that silver-coated rose petals and taro leaves are highly efficient SERS substrates.[50,51] Here, we find that the Au-coated PDMS reed leaf are also SERS active substrates because the Au-coated reed leaf possesses hierarchical micronanostructures all over the surface. Additionally, after Au coating, a highly dense Au island film is formed on the surface (Figure 5a). The as-formed plasmonic structures may help in the enhancement of the local electromagnetic field and achieve high SERS activity. To investigate the SERS detection ability of the Au-coated PDMS reed leaf, we employed Rhodamine 6G (R6G) as the probe molecule and quantitatively evaluated the SERS enhancement. Figure 5b shows the SERS spectra of R6G within the concentration range of 10^{-5} to 10^{-10} M. As observed from the SERS spectra, typical bands of R6G (at 617, 718, 1189, and 1362 cm^{-1}) can be identified, indicating the good SERS enhancement and the low detection limit. Because the SERS substrate is soft and flexible, the SERS enhancement can be further tuned by bending the substrate (Figure S5). Taking advantage of the uniform micronanostructures of natural reed leaves, our SERS sensor also demonstrated reasonable reproducibility. We randomly detected 50 different points from the Au-coated PDMS reed leaf. These 50 SERS spectra show reasonable homogeneity. By measuring the peaks at 617, 718, 1189, and 1362 cm^{-1}, we found that the SERS signals are reproducible. (Figure 5c). As compared with other soft SERS substrates,[52,53] our Au-coated PDMS reed leaf shows reasonable performance (Table S2). Using the capacitive sensor as the SERS substrate, we demonstrated the SERS detection of human sweat (Figure 5d). Typical bands of lactic acid (1170, 1475 cm^{-1}), fatty acids (1270 cm^{-1}), and urea (1030 cm^{-1}) can be detected from the sweat sample. The combination of wearable electronics with SERS may provide the possibility for SERS detection of human metabolites. However, to achieve quantitative detection of special metabolites toward clinical diagnosis, it remains a big challenge. First, the complexity of metabolites would make the analysis of SERS spectra quite difficult. Moreover, the SERS detection mode might be incompatible with general wearable devices. For instance, it needs a Raman spectrometer that might be not wearable.

■ CONCLUSIONS

In conclusion, using natural reed leaves as templates, we have prepared a capacitive sensor with biomimetic micronanostructures on the PDMS elastomer. The device structure of our capacitive sensor is very simple. Two thin layers of Au coating on the front side (with micronanostructures) and the back side (planar structure) of the PDMS reed leaf can serve as electrodes, and the PDMS leaf acts as a deformable dielectric layer. The capacitive sensor demonstrated high sensitivity (0.6 kPa^{-1}) in the low-pressure region and fast response/recovery time (180/120 ms). It enables detection of multimodal signals, including tiny forces (e.g., wrist pulses and acoustic vibrations at throat), motion of fingers, and proximity, and can serve as SERS substrates for the detection of the metabolites in sweat because of the natural plasmonic structures after Au coating. The natural material-templating strategy would facilitate the fabrication of high-performance pressure sensors. In addition, the resultant versatile electronic skin that enables multi-physiological signal detection may have great potential for human health monitoring.

■ ASSOCIATED CONTENT

Supporting Information

The Supporting Information is available free of charge on the ACS Publications website at DOI: 10.1021/acsami.9b14135.

DOI: 10.1021/acsami.9b14135
ACS Appl. Mater. Interfaces 2019, 11, 38084−38091

Detection limit of the pressure sensor, schematic illustration of the proximity sensing mechanism, capacitive changes versus the distance of the grounded metal rod, capacitive changes versus the distance of the statically neutralized metal rod, capacitance variations of the strain sensor versus the bending curvature, detection limit of the strain sensor, Raman spectra of R6G measured on planar and bended substrates, table of sensing performance comparison of some similar sensors, and a table of SERS performance comparison of some typical soft SERS substrates (PDF)

AUTHOR INFORMATION

Corresponding Author

*E-mail: yonglaizhang@jlu.edu.cn (Y.-L.Z.).

ORCID

Yong-Lai Zhang: 0000-0002-4282-250X

Hong-Bo Sun: 0000-0003-2127-8610

Author Contributions

The manuscript was written through contributions of all authors. All authors have given approval to the final version of the manuscript.

Notes

The authors declare no competing financial interest.

ACKNOWLEDGMENTS

The authors acknowledge the National Key Research and Development Program of China and National Natural Science Foundation of China under grant nos. 2017YFB1104300, 61935008, 61775078, 61590930, and 61605055 for support. We also acknowledge the Natural Science Foundation of Jilin Province grant no. 20180101061JC.

REFERENCES

(1) Wang, L.; Chen, D.; Jiang, K.; Shen, G. New Insights and Perspectives into Biological Materials for Flexible Electronics. *Chem. Soc. Rev.* **2017**, *46*, 6764−6815.

(2) Wang, L.; Jackman, J. A.; Tan, E.-L.; Park, J. H.; Potroz, M. G.; Hwang, E. T.; Cho, N.-J. High-Performance, Flexible Electronic Skin Sensor Incorporating Natural Microcapsule Actuators. *Nano Energy* **2017**, *36*, 38−45.

(3) Wang, L.; Wang, K.; Lou, Z.; Jiang, K.; Shen, G. Plant-Based Modular Building Blocks for "Green" Electronic Skins. *Adv. Funct. Mater.* **2018**, *28*, 1804510.

(4) Schwartz, G.; Tee, B. C. K.; Mei, J. G.; Appleton, A. L.; Kim, D. H.; Wang, H. L.; Bao, Z. N. Flexible Polymer Transistors with High Pressure Sensitivity for Application in Electronic Skin and Health Monitoring. *Nat. Commun.* **2013**, *4*, 1859.

(5) Chen, S.; Wu, N.; Ma, L.; Lin, S.; Yuan, F.; Xu, Z.; Li, W.; Wang, B.; Zhou, J. Noncontact Heartbeat and Respiration Monitoring Based on a Hollow Microstructured Self-Powered Pressure Sensor. *ACS Appl. Mater. Interfaces* **2018**, *10*, 3660−3667.

(6) Zhu, B.; Ling, Y.; Yap, L. W.; Yang, M.; Lin, F.; Gong, S.; Wang, Y.; An, T.; Zhao, Y.; Cheng, W. Hierarchically Structured Vertical Gold Nanowire Array-Based Wearable Pressure Sensors for Wireless Health Monitoring. *ACS Appl. Mater. Interfaces* **2019**, *11*, 29014−29021.

(7) Wang, X.; Gu, Y.; Xiong, Z.; Cui, Z.; Zhang, T. Silk-Molded Flexible, Ultrasensitive, and Highly Stable Electronic Skin for Monitoring Human Physiological Signals. *Adv. Mater.* **2014**, *26*, 1336−1342.

(8) Chen, L. Y.; Tee, B. C. K.; Chortos, A. L.; Schwartz, G.; Tse, V.; Lipomi, D. J.; Wong, H. S. P.; McConnell, M. V.; Bao, Z. A. Continuous Wireless Pressure Monitoring and Mapping with Ultra-Small Passive Sensors for Health Monitoring and Critical Care. *Nat. Commun.* **2014**, *5*, 5028.

(9) Boutry, C. M.; Nguyen, A.; Lawal, Q. O.; Chortos, A.; Rondeau-Gagné, S.; Bao, Z. A Sensitive and Biodegradable Pressure Sensor Array for Cardiovascular Monitoring. *Adv. Mater.* **2015**, *27*, 6954−6961.

(10) Luo, N.; Dai, W.; Li, C.; Zhou, Z.; Lu, L.; Poon, C. C. Y.; Chen, S.-C.; Zhang, Y.; Zhao, N. Flexible Piezoresistive Sensor Patch Enabling Ultralow Power Cuffless Blood Pressure Measurement. *Adv. Funct. Mater.* **2016**, *26*, 1178−1187.

(11) Gao, W.; Emaminejad, S.; Nyein, H. Y. Y.; Challa, S.; Chen, K.; Peck, A.; Fahad, H. M.; Ota, H.; Shiraki, H.; Kiriya, D.; Lien, D.-H.; Brooks, G. A.; Davis, R. W.; Javey, A. Fully Integrated Wearable Sensor Arrays for Multiplexed in situ Perspiration Analysis. *Nature* **2016**, *529*, 509−514.

(12) Chortos, A.; Liu, J.; Bao, Z. Pursuing Prosthetic Electronic Skin. *Nat. Mater.* **2016**, *15*, 937−950.

(13) Liu, Z.; Ma, Y.; Ouyang, H.; Shi, B.; Li, N.; Jiang, D.; Xie, F.; Qu, D.; Zou, Y.; Huang, Y.; Li, H.; Zhao, C.; Tan, P.; Yu, M.; Fan, Y.; Zhang, H.; Wang, Z. L.; Li, Z. Transcatheter Self-Powered Ultrasensitive Endocardial Pressure Sensor. *Adv. Funct. Mater.* **2019**, *29*, 1807560.

(14) Yang, W.; Chen, J.; Wen, X.; Jing, Q.; Yang, J.; Su, Y.; Zhu, G.; Wu, W.; Wang, Z. L. Triboelectrification Based Motion Sensor for Human-Machine Interfacing. *ACS Appl. Mater. Interfaces* **2014**, *6*, 7479−7484.

(15) Jung, S.; Kim, J. H.; Kim, J.; Choi, S.; Lee, J.; Park, I.; Hyeon, T.; Kim, D.-H. Reverse-Micelle-Induced Porous Pressure-Sensitive Rubber for Wearable Human-Machine Interfaces. *Adv. Mater.* **2014**, *26*, 4825−4830.

(16) Lim, S.; Son, D.; Kim, J.; Lee, Y. B.; Song, J.-K.; Choi, S.; Lee, D. J.; Kim, J. H.; Lee, M.; Hyeon, T.; Kim, D.-H. Transparent and Stretchable Interactive Human Machine Interface Based on Patterned Graphene Heterostructures. *Adv. Funct. Mater.* **2015**, *25*, 375−383.

(17) Boutry, C. M.; Negre, M.; Jorda, M.; Vardoulis, O.; Chortos, A.; Khatib, O.; Bao, Z. A Hierarchically Patterned, Bioinspired E-Skin Able to Detect the Direction of Applied Pressure for Robotics. *Sci. Robot.* **2018**, *3*, No. eaau6914.

(18) Tee, B. C.-K.; Wang, C.; Allen, R.; Bao, Z. An Electrically and Mechanically Self-Healing Composite with Pressure- and Flexion-Sensitive Properties for Electronic Skin Applications. *Nat. Nanotechnol.* **2012**, *7*, 825−832.

(19) Larson, C.; Peele, B.; Li, S.; Robinson, S.; Totaro, M.; Beccai, L.; Mazzolai, B.; Shepherd, R. Highly Stretchable Electroluminescent Skin for Optical Signaling and Tactile Sensing. *Science* **2016**, *351*, 1071−1074.

(20) Zhong, Q.; Zhong, J.; Cheng, X.; Yao, X.; Wang, B.; Li, W.; Wu, N.; Liu, K.; Hu, B.; Zhou, J. Paper-Based Active Tactile Sensor Array. *Adv. Mater.* **2015**, *27*, 7130−7136.

(21) Lv, L.; Zhang, P.; Xu, T.; Qu, L. Ultrasensitive Pressure Sensor Based on an Ultralight Sparkling Graphene Block. *ACS Appl. Mater. Interfaces* **2017**, *9*, 22885−22892.

(22) Kim, Y.; Na, J.; Park, C.; Shin, H.; Kim, E. PEDOT as a Flexible Organic Electrode for a Thin Film Acoustic Energy Harvester. *ACS Appl. Mater. Interfaces* **2015**, *7*, 16279−16286.

(23) Sheng, L.; Liang, Y.; Jiang, L.; Wang, Q.; Wei, T.; Qu, L.; Fan, Z. Bubble-Decorated Honeycomb-Like Graphene Film as Ultrahigh Sensitivity Pressure Sensors. *Adv. Funct. Mater.* **2015**, *25*, 6545−6551.

(24) Jason, N. N.; Ho, M. D.; Cheng, W. Resistive Electronic Skin. *J. Mater. Chem. C* **2017**, *5*, 5845−5866.

(25) Liu, Y.-Q.; Zhang, Y.-L.; Jiao, Z.-Z.; Han, D.-D.; Sun, H.-B. Directly Drawing High-Performance Capacitive Sensors on Copying Tissues. *Nanoscale* **2018**, *10*, 17002−17006.

(26) Nie, B.; Li, R.; Cao, J.; Brandt, J. D.; Pan, T. Flexible Transparent Iontronic Film for Interfacial Capacitive Pressure Sensing. *Adv. Mater.* **2015**, *27*, 6055−6062.

(27) Lipomi, D. J.; Vosgueritchian, M.; Tee, B. C.-K.; Hellstrom, S. L.; Lee, J. A.; Fox, C. H.; Bao, Z. Skin-Like Pressure and Strain

Sensors Based on Transparent Elastic Films of Carbon Nanotubes. *Nat. Nanotechnol.* **2011**, *6*, 788−792.
(28) Gao, N. W.; He, Y. L.; Tao, X. L.; Xu, X. Q.; Wu, X.; Wang, Y. P. Crystal-Confined Freestanding Ionic Liquids for Reconfigurable and Repairable Electronics. *Nat. Commun.* **2019**, *10*, 547.
(29) He, Y.; Gui, Q.; Wang, Y.; Wang, Z.; Liao, S.; Wang, Y. A Polypyrrole Elastomer Based on Confined Polymerization in a Host Polymer Network for Highly Stretchable Temperature and Strain Sensors. *Small* **2018**, *14*, 1800394.
(30) He, Y.; Liao, S.; Jia, H.; Cao, Y.; Wang, Z.; Wang, Y. A Self-Healing Electronic Sensor Based on Thermal-Sensitive Fluids. *Adv. Mater.* **2015**, *27*, 4622−4627.
(31) Osica, I.; Imamura, G.; Shiba, K.; Ji, Q.; Shrestha, L. K.; Hill, J. P.; Kurzydłowski, K. J.; Yoshikawa, G.; Ariga, K. Highly Networked Capsular Silica-Porphyrin Hybrid Nanostructures as Efficient Materials for Acetone Vapor Sensing. *ACS Appl. Mater. Interfaces* **2017**, *9*, 9945−9954.
(32) Pang, C.; Lee, G.-Y.; Kim, T.-i.; Kim, S. M.; Kim, H. N.; Ahn, S.-H.; Suh, K.-Y. A Flexible and Highly Sensitive Strain-Gauge Sensor Using Reversible Interlocking of Nanofibres. *Nat. Mater.* **2012**, *11*, 795−801.
(33) Pan, L. J.; Chortos, A.; Yu, G. H.; Wang, Y. Q.; Isaacson, S.; Allen, R.; Shi, Y.; Dauskardt, R.; Bao, Z. N. An Ultra-Sensitive Resistive Pressure Sensor Based on Hollow-Sphere Microstructure Induced Elasticity in Conducting Polymer Film. *Nat. Commun.* **2014**, *5*, 3002.
(34) Ji, Q.; Honma, I.; Paek, S.-M.; Akada, M.; Hill, J. P.; Vinu, A.; Ariga, K. Layer-by-Layer Films of Graphene and Ionic Liquids for Highly Selective Gas Sensing. *Angew. Chem., Int. Ed.* **2010**, *49*, 9737−9739.
(35) Choong, C.-L.; Shim, M.-B.; Lee, B.-S.; Jeon, S.; Ko, D.-S.; Kang, T.-H.; Bae, J.; Lee, S. H.; Byun, K.-E.; Im, J.; Jeong, Y. J.; Park, C. E.; Park, J.-J.; Chung, U.-I. Highly Stretchable Resistive Pressure Sensors Using a Conductive Elastomeric Composite on a Micropyramid Array. *Adv. Mater.* **2014**, *26*, 3451−3458.
(36) She, X. Y.; Shen, Y.; Wang, J. F.; Jin, C. J. Pd Films on Soft Substrates: A Visual, High-Contrast and Low-Cost Optical Hydrogen Sensor. *Light Sci. Appl.* **2019**, *8*, 4.
(37) Park, J.; Lee, Y.; Hong, J.; Ha, M.; Jung, Y.-D.; Lim, H.; Kim, S. Y.; Ko, H. Giant Tunneling Piezoresistance of Composite Elastomers with Interlocked Microdome Arrays for Ultrasensitive and Multimodal Electronic Skins. *ACS Nano* **2014**, *8*, 4689−4697.
(38) Yesilkoy, F.; Terborg, R. A.; Pello, J.; Belushkin, A. A.; Jahani, Y.; Pruneri, V.; Altug, H. Phase-Sensitive Plasmonic Biosensor Using a Portable and Large Field-of-View Interferometric Microarray Imager. *Light Sci. Appl.* **2018**, *7*, 17152.
(39) Zhang, Y.-L.; Chen, Q.-D.; Xia, H.; Sun, H.-B. Designable 3D nanofabrication by femtosecond laser direct writing. *Nano Today* **2010**, *5*, 435−448.
(40) Liu, K.; Yao, X.; Jiang, L. Recent Developments in Bio-Inspired Special Wettability. *Chem. Soc. Rev.* **2010**, *39*, 3240−3255.
(41) Liu, K.; Tian, Y.; Jiang, L. Bio-Inspired Superoleophobic and Smart Materials: Design, Fabrication, and Application. *Prog. Mater. Sci.* **2013**, *58*, 503−564.
(42) Yin, K.; Dong, X.; Zhang, F.; Wang, C.; Duan, J. a. Superamphiphobic Miniature Boat Fabricated by Laser Micromachining. *Appl. Phys. Lett.* **2017**, *110*, 121909.
(43) Liu, Y.-Q.; Zhang, Y.-L.; Fu, X.-Y.; Sun, H.-B. Bioinspired Underwater Superoleophobic Membrane Based on a Graphene Oxide Coated Wire Mesh for Efficient Oil/Water Separation. *ACS Appl. Mater. Interfaces* **2015**, *7*, 20930−20936.
(44) Shi, J.; Wang, L.; Dai, Z.; Zhao, L.; Du, M.; Li, H.; Fang, Y. Multiscale Hierarchical Design of a Flexible Piezoresistive Pressure Sensor with High Sensitivity and Wide Linearity Range. *Small* **2018**, *14*, 1800819.
(45) Han, B.; Zhang, Y. L.; Zhu, L.; Li, Y.; Ma, Z. C.; Liu, Y. Q.; Zhang, X. L.; Cao, X. W.; Chen, Q. D.; Qiu, C. W.; Sun, H. B. Plasmonic-Assisted Graphene Oxide Artificial Muscles. *Adv. Mater.* **2019**, *31*, 1806386.
(46) Su, B.; Gong, S.; Ma, Z.; Yap, L. W.; Cheng, W. Mimosa-Inspired Design of a Flexible Pressure Sensor with Touch Sensitivity. *Small* **2015**, *11*, 1886−1891.
(47) Yin, K.; Yang, S.; Dong, X.; Chu, D.; Gong, X.; Duan, J.-A. Femtosecond Laser Fabrication of Shape-Gradient Platform: Underwater Bubbles Continuous Self-Driven and Unidirectional Transportation. *Appl. Surf. Sci.* **2019**, *471*, 999−1004.
(48) Jiang, H.-B.; Liu, Y.-Q.; Zhang, Y.-L.; Liu, Y.; Fu, X.-Y.; Han, D.-D.; Song, Y.-Y.; Ren, L.; Sun, H.-B. Reed Leaf-Inspired Graphene Films with Anisotropic Superhydrophobicity. *ACS Appl. Mater. Interfaces* **2018**, *10*, 18416−18425.
(49) Jian, M.; Xia, K.; Wang, Q.; Yin, Z.; Wang, H.; Wang, C.; Xie, H.; Zhang, M.; Zhang, Y. Flexible and Highly Sensitive Pressure Sensors Based on Bionic Hierarchical Structures. *Adv. Funct. Mater.* **2017**, *27*, 1606066.
(50) Xu, B.-B.; Zhang, Y.-L.; Zhang, W.-Y.; Liu, X.-Q.; Wang, J.-N.; Zhang, X.-L.; Zhang, D.-D.; Jiang, H.-B.; Zhang, R.; Sun, H.-B. Silver-Coated Rose Petal: Green, Facile, Low-Cost and Sustainable Fabrication of a SERS Substrate with Unique Superhydrophobicity and High Efficiency. *Adv. Opt. Mater.* **2013**, *1*, 56−60.
(51) Huang, J.-A.; Zhang, Y.-L.; Zhao, Y.; Zhang, X.-L.; Sun, M.-L.; Zhang, W. Superhydrophobic SERS Chip Based on a Ag Coated Natural Taro-Leaf. *Nanoscale* **2016**, *8*, 11487−11493.
(52) Si, K. J.; Guo, P.; Shi, Q.; Cheng, W. Self-Assembled Nanocube-Based Plasmene Nanosheets as Soft Surface-Enhanced Raman Scattering Substrates toward Direct Quantitative Drug Identification on Surfaces. *Anal. Chem.* **2015**, *87*, 5263−5269.
(53) Chen, Y.; Si, K. J.; Sikdar, D.; Tang, Y.; Premaratne, M.; Cheng, W. Ultrathin Plasmene Nanosheets as Soft and Surface-Attachable SERS Substrates with High Signal Uniformity. *Adv. Opt. Mater.* **2015**, *3*, 919−924.

DOI: 10.1021/acsami.9b14135
ACS Appl. Mater. Interfaces 2019, 11, 38084−38091